An infra-red study of conformational changes occurring during the drawing of PEMT, PET and PEMT/PET copolymer

P. Spiby, M. A. O'Neill*, R. A. Duckett and I. M. Ward†
IRC in Polymer Science and Technology, University of Leeds, Leeds LS2 9JT, UK
(Received 29 July 1991; revised 28 November 1991; accepted 16 December 1991)

An i.r. study has been made of the conformational transitions which accompany the tensile drawing of poly(ethylene terephthalate) (PET) and the non-crystallizing polyesters, poly(ethylene methyl terephthalate) (PEMT) and a 60/40 PEMT/PET copolymer. For a given level of overall orientation, measured by birefringence, the *gauche* conformers were converted into *trans* more effectively and the *trans* conformers were more highly oriented in PET than in PEMT or the copolymer. The *gauche/trans* conformational change also occurred more effectively in hot drawing compared with cold drawing for PEMT and its copolymer. These differences in drawing behaviour were reflected in the development of elastic modulus with molecular orientation in these materials.

(Keywords: infra-red; conformational changes; PET; PEMT)

INTRODUCTION

It is now well-established that the tensile drawing of poly(ethylene terephthalate) (PET) involves essentially three major factors: molecular orientation; changes in molecular conformation (e.g. *trans/gauche* conformers associated with the glycol residue); and crystallization. In an attempt to gain an understanding of the first two factors, in the absence of the third, we have undertaken studies of the non-crystallizing polyester, poly(ethylene methyl terephthalate) (PEMT). In a previous publication[1], the stress-optical behaviour of this polymer has been reported and was shown to be similar to that for PET.

The present paper describes a comparative study of the development of molecular orientation in PET, PEMT and a 60/40 copolymer of PEMT and PET, which also does not crystallize. The primary thrust of this study is the use of i.r. spectroscopy to determine the *trans/gauche* conformational changes in conjunction with optical measurements of overall molecular orientation. Measurements of mechanical modulus will also be reported, together with their relationship to the i.r. and optical data.

EXPERIMENTAL

The preparations of the PEMT and the 60/40 copolymer of PEMT/PET have been described in detail[1]. It was confirmed by WAXS studies that both the homopolymer and the copolymer showed no crystallinity. Further details of these polymers are given in *Table 1*.

For the i.r. and optical measurements narrow oriented tapes were produced. As described previously, tapes of 255 μm × 1.0 mm cross-section were prepared by melt spinning. These low orientation tapes were then drawn to a series of draw ratios in a controlled temperature bath between two rollers, whose relative angular velocities determine the draw ratio. Draw temperatures of 56 and 70°C were used for PEMT and 63.5 and 75°C for the 60/40 copolymer.

For the comparative measurements on PET, an amorphous film (supplied by E.I. du Pont de Nemours) was drawn at 80°C at a cross-head speed of 2 cm min^{-1} to a series of draw ratios using a tensile testing machine (RPD Howden Ltd).

Refractive index measurements

The two refractive indices in the plane of the film n_z and n_x were measured using a Zeiss Interphako interference microscope as described in a previous publication[2]. The assumption of transverse isotropy was confirmed by using the measured values to calculate a value for the refractive index of the isotropic polymer n_i using equation (1):

$$\frac{n_i^2-1}{n_i^2+2}=\frac{1}{3}\frac{d_i}{d_o}\left[\frac{(n_z^2-1)}{(n_z^2+2)}+\frac{2(n_x^2-1)}{(n_x^2+2)}\right] \quad (1)$$

where d_i and d_o are the densities of the isotropic and oriented polymer, respectively.

In all cases the calculated value for n_i agreed with the experimental values for PET, PEMT and the copolymer, respectively, to within 0.0002.

The optical orientation function $\langle P_2(\cos\theta)\rangle_{opt}$ was calculated from the measured birefringence $\Delta n\ (=n_z-n_x)$ and an estimate of the intrinsic birefringence $\Delta n_{max}=0.20$,

*Now at ICI Films Group, Wilton, UK
†To whom correspondence should be addressed

0032-3861/92/214479-07

Table 1 Details of the polymers studied

Polymer	Intrinsic viscosity ($cm^3\ g^{-1}$)	T_g (°C)
PEMT	0.67	61
60/40 PEMT/PET	0.58	68
PET	0.62	80

0.215 and 0.235 for PEMT, the copolymer and PET, respectively, obtained from the assumption of additivity of bond polarizabilities as follows:

$$\langle P_2(\cos\theta)\rangle_{opt} = \Delta n/\Delta n_{max} \quad (2)$$

The value of Δn_{max} for PEMT is significantly different from that used in reference 1 ($\Delta n_{max} = 0.144$) which appeared to give a good fit to birefringence/draw ratio data using the aggregate model.

I.r. measurements

The polarized i.r. spectra of the PEMT and copolymer samples were recorded at ICI Wilton using a Nicolet Instruments 170SX *FT*i.r. spectrometer. When the spectra were analysed, using digital differentiation techniques, it was noticed that all the spectra had harmonic variations in the absorption background. The harmonic variation was shifted in phase and amplitude in the neighbourhood of absorption peaks. These variations in background are consistent with interference between multiple reflections from the front and back surfaces of the sample. The spectra of the PET samples were recorded at Leeds using a Perkin-Elmer PE580-B i.r. spectrophotometer. These samples were held between KBr plates and immersed in a mulling agent (liquid paraffin) to remove the interference fringes from the spectra.

The i.r. spectra of PEMT and PET are shown in *Figures 1a* and *b*, respectively. It can be seen that the spectra are similar in many respects: in particular, in the region 1770–1250 cm^{-1}, the spectra are almost identical. However, in the region 1050–600 cm^{-1} the two spectra are very different. In previous research[3] the 'low' wavenumber region was used for quantitative measurements of the *trans* and *gauche* absorption: for PEMT new procedures have been devised based on the 'high' wavenumber region.

The curve fitting procedures adopted in this investigation are similar to those devised by Hutchinson[4] and reported in detail previously[5]: the i.r. spectra in the region 1070–770 cm^{-1} were fitted to a series of Lorentzian-shaped bands of fixed position and halfwidth. *Figures 2a* and *b* show the results of a similar procedure for PEMT and PET, respectively, in the region 1520–1300 cm^{-1}. Following band assignments for PET which have been established in several previous studies[6], the bands at 1337, 1340 and 1344 cm^{-1} are assigned to CH_2 'wagging' modes for the *trans* glycol conformation and 1367, 1370 and 1375 cm^{-1} to the corresponding *gauche* conformation.

A simplified version of the approach used by Cunningham *et al.*[7] was used to convert the Lorentzian line shapes to 'true' absorption values due to the difficulty of removing the background effects caused by interference. No corrections were made for losses due to surface reflections.

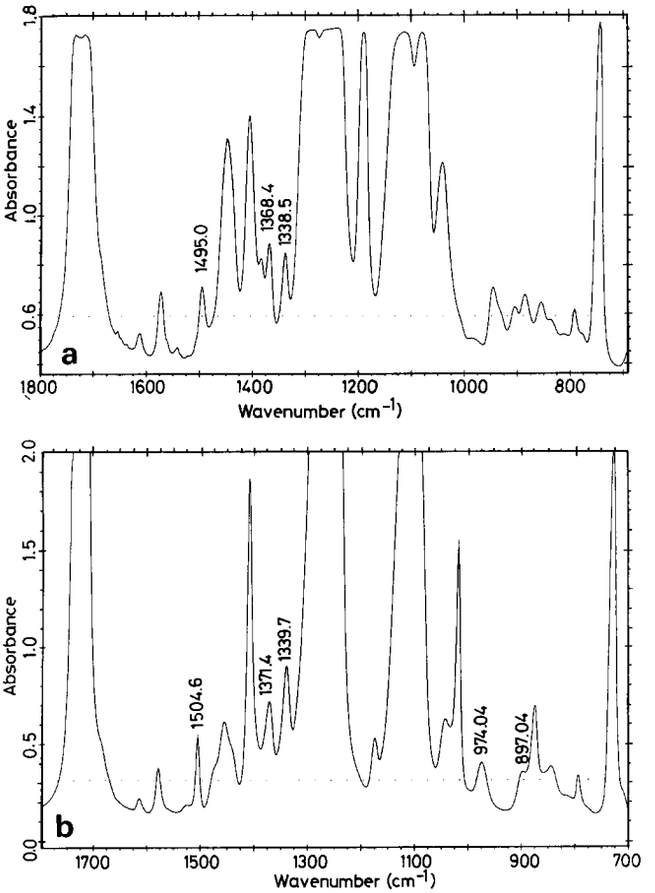

Figure 1 Typical i.r. spectra for (a) PEMT and (b) PET

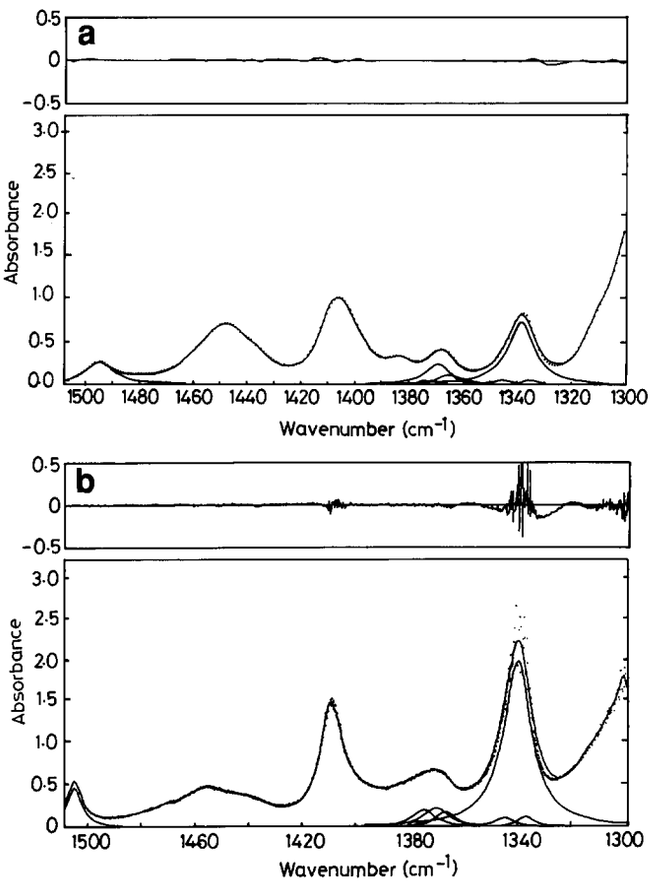

Figure 2 Typical computer fits to i.r. spectra for (a) PEMT and (b) PET. The top curves show the deviations between the fitted curves and the experimental data in each case

The equations used were as follows:

$$A \simeq 0.4343\ 4\pi\bar{\nu}kt \tag{3}$$

$$\phi' \simeq \frac{6nk}{(n^2+2)^2} \tag{4}$$

$$\phi = \frac{\pi}{2}\phi'\Delta \tag{5}$$

where A is the measured absorbance, $\bar{\nu}$ is the wavelength of the i.r. absorption index, k is the imaginary part of the complex refractive index, t is the sample thickness (see below), n is the real part of the complex refractive index ($n \simeq n_{opt}$) and Δ is the halfwidth of the absorption peak. The parameter ϕ' is effectively the intrinsic peak absorbance and ϕ the area under the absorption peak.

The curve fitting procedures returned values for A and Δ for each absorption process. These parameters, together with the optical refractive index n_{opt} and sample thickness t, were used to calculate the volume polarizability ϕ.

Finally the ϕ values were used to calculate

$$N\langle\alpha''\rangle = \frac{3}{4\pi}\phi \tag{6}$$

where N is the number of absorbing species per unit volume and $\langle\alpha''\rangle$ is the imaginary part of the average polarizability for the appropriate vibration mode.

Because of the uniaxial symmetry of the drawn tapes it was necessary to record spectra both with the electric vector of the polarized i.r. radiation parallel to the draw direction – leading to a value ϕ_z for the volume polarizability and with the electric vector perpendicular to the draw direction for ϕ_x.

Following previous work the orientation of individual conformers was calculated from

$$\frac{\phi_z - \phi_x}{(\phi_z + 2\phi_x)} = P_2(\theta_m)\langle P_2(\theta)\rangle_{i.r.} \tag{7}$$

where $P_2(\theta_m) = 1/2(3\cos^2\theta_m - 1)$, θ_m is the angle between the transition moment vector and the unit direction, and $\langle P_2(\theta)\rangle_{i.r.} = 1/2(3\langle\cos^2\theta\rangle - 1)$, where θ is the angle between the unit direction and the draw direction, and the angular brackets represent an ensemble average.

Thickness measurement

Detailed quantitative analysis of the i.r. spectra requires accurate knowledge of sample thickness at the position traversed by the i.r. beam. The small thickness of the films used ($\sim 5\,\mu m$) and observations of fluctuations in thickness made direct measurement of sample thickness unreliable. Following previous papers an 'internal thickness calibration' was used based on the i.r. absorption for a vibration mode which was not conformation sensitive. The band used for this was the 1505 cm^{-1} benzene ring vibration which, when suitably averaged to compensate for dichroism, gave an excellent correlation with thickness for the PET spectra. (In PEMT the absorption peak moves to 1495 cm^{-1} due to the influence of the methyl group but this does not seriously compromise the method.) This technique has the advantage that the film thickness is measured at exactly the place at which the i.r. analysis is to be made.

The method of calculation used for the thickness calibration is as follows:

1. The area under the 1505 cm^{-1} (or 1495 cm^{-1}) peak, suitably averaged to compensate for dichroism by calculating $\phi_o = (\phi_z + 2\phi_x)/3$, was calculated for each of a wide range of PET samples with known thickness and density using equations (3)–(5), but assuming a nominal thickness of 1 μm.
2. The product $(N\langle\alpha''\rangle)_{apparent}$ was calculated for each sample using equation (6). (Note that the actual value of $N\langle\alpha''\rangle$ is constant for all samples.)
3. A graph was plotted of relative thickness (i.e. measured thickness × density) *versus* $(N\langle\alpha''\rangle)_{apparent}$ for all samples.
4. For any other sample the product $(N\langle\alpha''\rangle)_{apparent}$ was calculated as in steps 1 and 2 and the relative thickness then read off the graph produced in step 3.

Mechanical measurements

The influence of molecular orientation on mechanical properties was monitored by measurement of a 10 s isochronal tensile creep modulus using an apparatus similar to that described by Gupta and Ward[8].

RESULTS AND DISCUSSION

I.r. spectroscopy

Previous work using i.r. analysis of conformational changes in PET induced by drawing concentrated on the spectral region from 1070 to 770 cm^{-1}. It was established that absorption bands in the 889–906 cm^{-1} region could be assigned to *gauche* conformers, whereas the 962–979 cm^{-1} region is associated with *trans* conformers. Spectral reconstruction techniques confirmed that the sum of the areas associated with Lorentzian bands at 962, 973 and 979 cm^{-1} is a measure of the *trans* content whereas the two Lorentzians at 889 and 899 cm^{-1} reflect the *gauche* content. On changing the polymer to PEMT these spectral regions change significantly so that they can no longer be used. Alternative absorption bands at 1337, 1340 and 1344 cm^{-1} were therefore identified as the *trans* bands and 1367, 1370 and 1375 cm^{-1} as *gauche* bands, and these absorptions were also present in PEMT and the 60:40 PEMT/PET copolymer. *Figures 3a* and *b* show the excellent correlation between the two types of *trans* band and two types of *gauche* band, respectively. With this confirmation the subsequent discussion relates to the 1337, 1340 and 1344 cm^{-1} bands for measurements of *trans* content and to the 1367, 1370 and 1375 cm^{-1} bands for measurements of *gauche* content, i.e.

$$\phi_{1337} + \phi_{1340} + \phi_{1344} = \phi_o^T$$

and

$$\phi_{1367} + \phi_{1370} + \phi_{1375} = \phi_o^G$$

Since $\phi^T \propto N^T\langle\alpha''\rangle^T$ and $\phi^G \propto N^G\langle\alpha''\rangle^G$ and $N^T + N^G$ is a constant, independent of orientation, a plot of ϕ_o^G *versus* ϕ_o^T is linear and leads to the value of $\langle\alpha''\rangle^T/\langle\alpha''\rangle^G = 0.84 \pm 0.09$. Using this value the fractional *trans* content $X^T = N^T/(N^T + N^G)$ and *gauche* content $X^G = N^G/(N^T + N^G)$ were calculated.

Figures 4–6 provide a comparison of the changes in *trans/gauche* conformational content as a function of

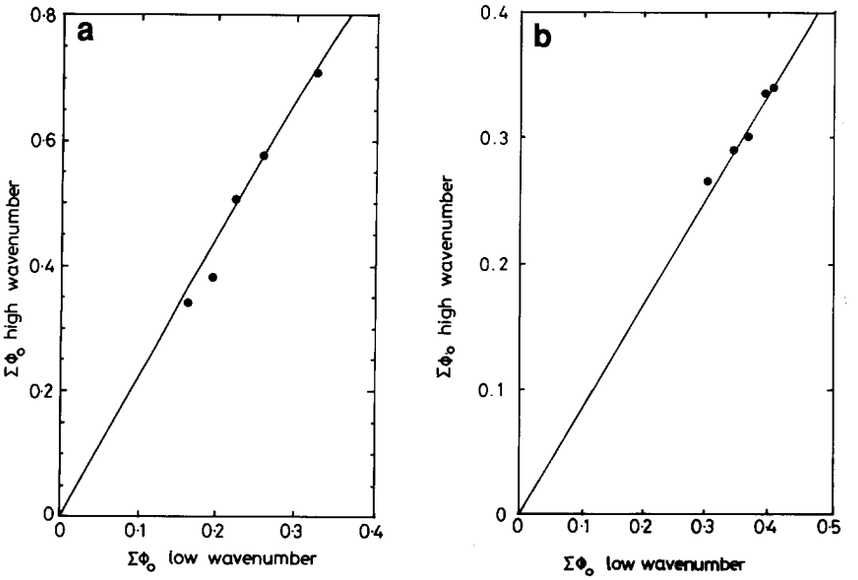

Figure 3 Calibration of conformer content measured using the 'high' and 'low' regions of the PET spectra: (a) total *trans*; (b) total *gauche*

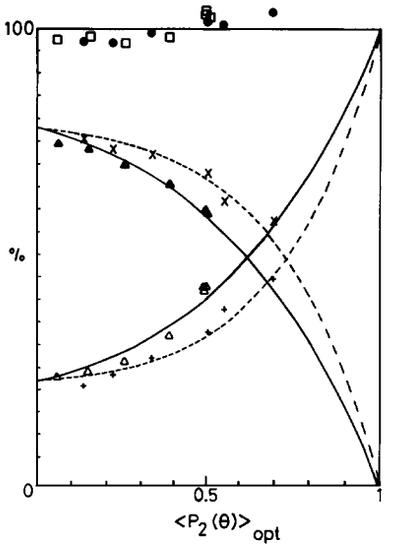

Figure 4 Variation of conformer concentrations with chain (optical) orientation in PEMT. Hot: (△) *trans*; (▲) *gauche*; (□) sum. Cold: (+) *trans*; (×) *gauche*; (●) sum

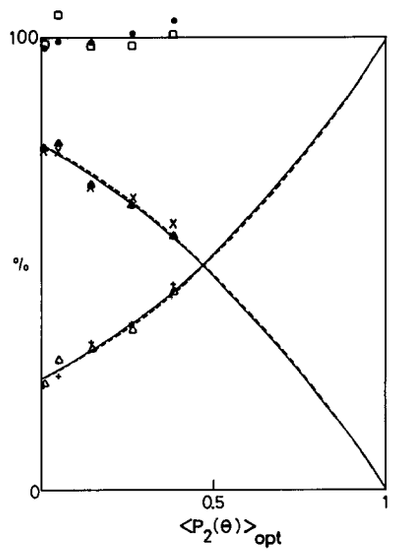

Figure 5 Variation of conformer concentrations with chain (optical) orientation in PET. Symbols as in *Figure 4*

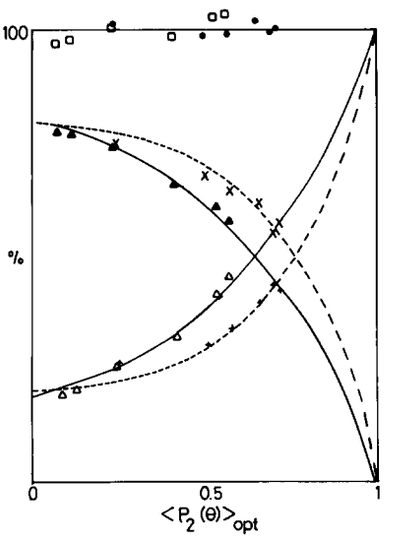

Figure 6 Variation of conformer concentrations with chain (optical) orientation in the 60:40 PEMT/PET copolymer. Symbols as in *Figure 4*

overall molecular orientation, the latter determined from the refractive index measurements. The comparison between hot drawn and cold drawn PEMT in *Figure 4* is of particular interest, and indicates that there is a restriction in the conversion of *gauche* conformers to *trans* in cold drawing compared with hot drawing. This suggests that the increased drawing stress at lower temperatures does not compensate for the loss in molecular mobility. The stress-optical studies reported previously suggested that whereas the development of molecular orientation in hot drawing can be very well modelled by the deformation of a molecular network, drawing below the glass transition temperature (T_g) is better described by the pseudo-affine deformation scheme, where the symmetry axes of the structure are rotated towards the draw direction as lines connecting pairs of points undergoing uniaxial deformation at constant volume. The present results show that conformational changes do take place even during drawing below T_g, presumably to accommodate the

required changes in length of the molecular chains. This observation, together with the fact that the maximum birefringence obtained experimentally is so much less than the value of Δn_{max} calculated from bond polarizabilities, suggests that further work is necessary to understand the development of orientation during cold drawing.

Comparison between hot drawn PEMT and hot drawn PET (*Figures 4* and *5*) shows that in PEMT a higher overall molecular orientation is obtained for a given *trans/gauche* ratio. We believe that this result is due to the positive contribution of *gauche* conformers in PEMT to the overall molecular orientation. (In PET, previous studies have shown that the *gauche* conformations make a negligible contribution to the overall molecular orientation, except at the lowest levels of orientation[3].) This is based on direct measurements of the orientation of the conformers as described above. However, interpretation of the values of $P_2(\theta_m^T)\langle P_2(\theta)\rangle^T$ and $P_2(\theta_m^G)\langle P_2(\theta)\rangle^G$ is difficult because of our lack of knowledge about the angles θ_m^T and θ_m^G. Since for PET the contribution to molecular orientation from the *gauche* conformers is effectively negligible it follows that

$$\langle P_2(\theta)\rangle_{i.r.} \simeq X^T\langle P_2(\theta)\rangle_{i.r.}^T \qquad (8)$$

Figure 7 reveals that a graph of $X^T P_2(\theta_m^T)\langle P_2(\theta)\rangle_{i.r.}^T$

$$\left[= X^T\left(\frac{\phi_z - \phi_x}{\phi_z + 2\phi_x}\right)\right]$$

from the 975 cm^{-1} vibration *versus* $\langle P_2(\theta)\rangle_{opt}$ is linear and from the slope a value of $\theta_m = 34°$ can be calculated. In *Figure 8* a plot of $X^T P_2(\theta_m^T)\langle P_2(\theta)\rangle_{i.r.}^T$ (for the 1340 cm^{-1} bands) *versus* $X^T P_2(\theta_m^T)\langle P_2(\theta)\rangle_{i.r.}^T$ (for the 975 cm^{-1} bands) is linear and from the slope a value of $\theta_m = 21°$ can be calculated for the 1340 cm^{-1} vibrations. Hence it is possible to calculate values for $\langle P_2(\theta)\rangle^T$ for the *trans* bands in the 1340 cm^{-1} region for PEMT, PET and for the copolymer assuming the same value of θ_m for each polymer and these are plotted *versus* $\langle P_2(\theta)\rangle_{opt}$ in *Figure 9*.

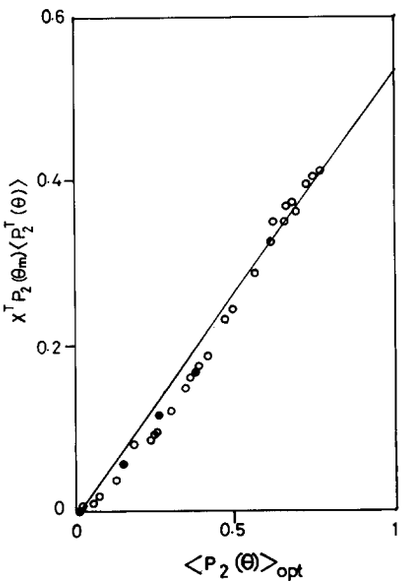

Figure 7 Contribution for PET of *trans* conformers to overall orientation assessed from the 'low' region of spectra *versus* optical orientation. The slope of the line leads to a value for the dipole orientation angle $\theta_m^T \sim 34°C$ in PET (see text). (●) this study; (○) from reference 5

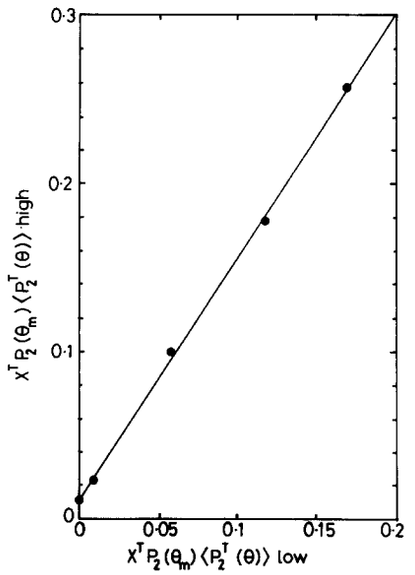

Figure 8 The *trans* contribution assessed via the 'high' and 'low' regions of the spectra. The slope leads to a value of $\theta_m \simeq 21°$ for the 'high' wavenumber absorption

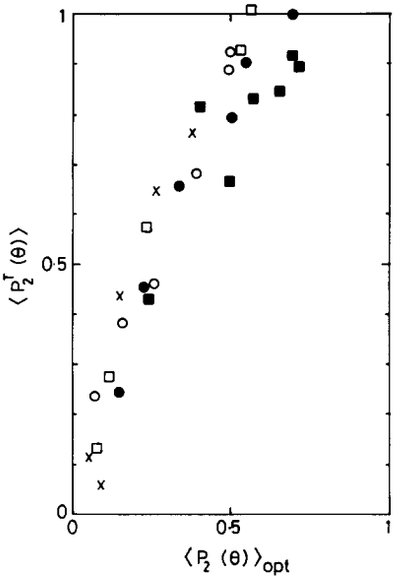

Figure 9 Orientation of *trans* conformers is seen to be higher than overall orientation, especially for hot drawn polymers: (×) high wavenumber PET; (○) hot drawn PEMT; (●) cold drawn PEMT; (□) hot drawn copolymer; (■) cold drawn copolymer

It can be seen that there are differences between the different polymers in that the orientation of the *trans* conformers is greater for PET than for PEMT. Because of the differences in *trans/gauche* ratios already noted, these differences between PET and PEMT are clearly brought out by the plots of $X^T\langle P_2(\theta)\rangle^T$ and $X^G P_2(\theta_m^G)\langle P_2(\theta)\rangle^G$ *versus* $\langle P_2(\theta)\rangle_{opt}$ shown in *Figures 10* and *11*. We can now see a clear reduction in the *trans* contribution to overall molecular orientation for PEMT compared with PET (*Figure 10*) and correspondingly an increased contribution from *gauche* conformers (*Figure 11*).

Young's modulus

In previous investigations of PET[5,9,10], it has invariably been found that there is an excellent

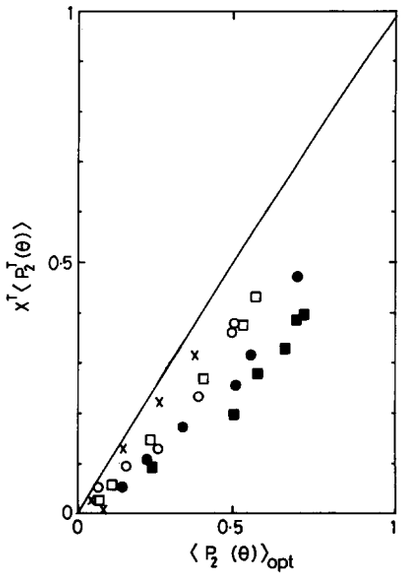

Figure 10 The *trans* contribution to orientation is indicated as a function of overall orientation. The contribution from *gauche* conformers is particularly large for the cold drawn materials. Symbols as in *Figure 9*

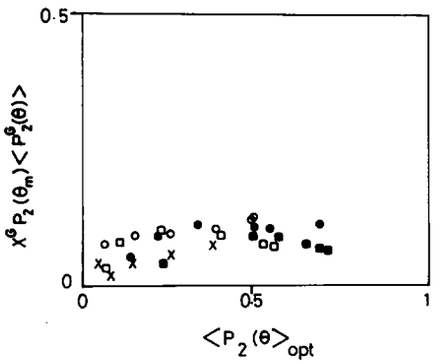

Figure 11 *Gauche* contribution to overall molecular orientation (see also *Figure 10*). Symbols as in *Figure 10*

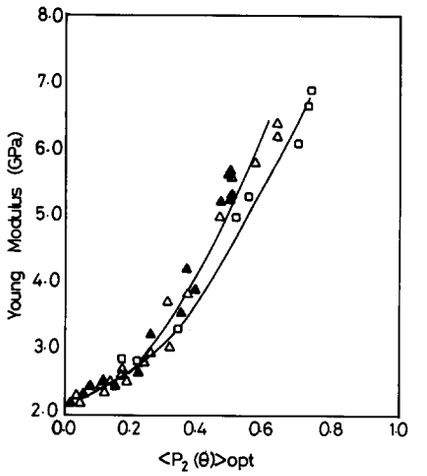

Figure 12 Variation of Young's modulus with overall orientation for PEMT: (△) 65°C; (▲) 70°C; (□) 56°C

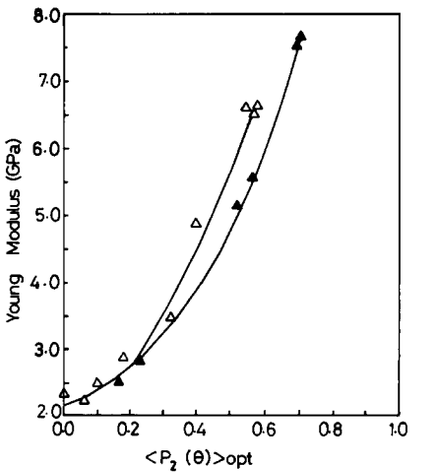

Figure 13 Variation of Young's modulus with overall orientation for PEMT/PET copolymer: (△) 75°C; (▲) 63.5°C

correlation between the Young's modulus of drawn fibres and the overall orientation, as determined from birefringence. Moreover this correlation was found to be independent of the drawing conditions, and even held for fibres where the molecular orientation was introduced at the melt-spinning stage by winding up at high speeds.

It can be seen from *Figures 12* and *13* that there is a distinct difference between the Young's modulus *versus* $\langle P_2(\theta)\rangle_{opt}$ curves for different draw temperatures in the case of both PEMT and the PEMT/PET copolymer. In particular, it can be seen that drawing at lower temperatures produces oriented materials with larger values of $\langle P_2(\theta)\rangle_{opt}$ for a given level of Young's modulus. This result is consistent with the observation that lower draw temperatures produce lower *trans*/*gauche* ratios for a given overall orientation and can be explained on the basis that in the case of PEMT and the copolymer, as distinct from PET, *gauche* conformations contribute to the overall orientation. However, their contribution to the modulus is expected to be small. In general terms the chain modulus of the *trans* conformation will be similar to that of the crystal i.e. ~100 GPa, whereas the chain modulus of the *gauche* conformation will be closer to the modulus of amorphous PET i.e. ~1 GPa, because it will involve bond angle rotations rather than bond bending and stretching.

CONCLUSIONS

The i.r. spectra provide valuable insight into the molecular mechanisms of deformation during the tensile drawing of PEMT, PET and a 60/40 PEMT/PET copolymer. In all three materials there is a conversion of *gauche* to *trans* conformers with increasing elongation, the process appearing to be more efficient during hot drawing.

Both *trans* and *gauche* conformers contribute to the overall orientation in PEMT, whereas in PET the *gauche* conformers appear to be only poorly oriented. The oriented *gauche* conformers in PEMT contribute significantly to the birefringence (and hence overall orientation) but make a negligible contribution to the Young's modulus. This destroys the correlation between Young's modulus and birefringence previously established with PET.

ACKNOWLEDGEMENTS

It is a pleasure to acknowledge the invaluable advice and assistance of Professor J. E. McIntyre and Dr A. H. Milburn of the Department of Textiles Industries, University of Leeds in the preparation of the PEMT and PEMT/PET copolymers. We also thank Dr M. MacKenzie and Mr N. Moore of ICI, Wilton for recording the i.r. spectra of the PEMT and PEMT/PET copolymers.

REFERENCES

1 O'Neill, M. A., Duckett, R. A. and Ward, I. M. *Polymer* 1988, **29**, 54
2 Perena, J. M., Duckett, R. A. and Ward, I. M. *J. Appl. Polym. Sci.* 1980, **25**, 1381
3 Hutchinson, I. J., Ward, I. M., Willis, H. A. and Zichy, V. *Polymer* 1980, **21**, 55
4 Hutchinson, I. J. *PhD Thesis* Leeds University, 1979
5 Yazdanian, M., Ward, I. M. and Brody, H. *Polymer* 1985, **26**, 1779
6 Wilding, M. A. and Ward, I. M. *Polymer* 1977, **18**, 327
7 Cunningham, A., Ward, I. M., Willis, H. A. and Zichy, V. *Polymer* 1974, **15**, 749
8 Gupta, V. B. and Ward, I. M. *J. Macromol. Sci. Phys.* 1967, **B1**, 373
9 Pinnock, P. R. and Ward, I. M. *Br. J. Appl. Phys.* 1964, **15**, 1559
10 Padibjo, S. R. and Ward, I. M. *Polymer* 1983, **24**, 1103